

Video rate near-field scanning optical microscopy

S. J. Bukofsky^{a)} and R. D. Grober

Department of Applied Physics, Yale University, New Haven, Connecticut 06520

(Received 4 June 1997; accepted for publication 12 September 1997)

The enhanced transmission efficiency of chemically etched near-field optical fiber probes makes it possible to greatly increase the scanning speed of near-field optical microscopes. This increase in system bandwidth allows sub-diffraction limit imaging of samples at video rates. We demonstrate image acquisition at 10 frames/s, rate-limited by mechanical resonances in our scanner. It is demonstrated that the optical signal to noise ratio is large enough for megahertz single pixel acquisition rates. © 1997 American Institute of Physics. [S0003-6951(97)04545-2]

Near-field scanning optical microscopy (NSOM) involves scanning a sub-wavelength sized aperture in close proximity to a sample.¹ Modern near-field probes are realized by fabricating tapered dielectric structures with sharp tips. The aperture is formed by shadow evaporation of aluminum on the walls of this dielectric tip. Since the inception of near-field optical microscopy, there has been a natural progression towards more efficient near-field probes. Early work by Pohl *et al.*² used tapered glass pipettes. Later, Betzig *et al.*³ employed probes made from optical fiber which had been heated and pulled to form a tapered structure.

Pulled fiber probes have apertures as small as 50 nm, but the optical throughput of such small apertures is of order 10^{-6} . As tips are made smaller, the efficiency worsens.⁴ In addition to low throughput, the maximum intensity that can be emitted from a near-field probe is limited to a few nanowatts, due to heat-induced probe damage. This small optical intensity manifests itself in the scanning speed of near-field instruments. Long integration times for good signal to noise ratio are the determining factor in scanning speed. Typical scanning speeds for near-field instruments are limited to less than 1 kHz pixel acquisition rates.

We have fabricated chemically etched near-field optical probes as described previously by Hoffmann *et al.*⁵ and Zeisel *et al.*⁶ These probes provide a thousandfold improvement in optical throughput over pulled probes. We currently make 70 nm diameter apertures with transmission efficiencies of 10^{-3} and microwatt transmitted optical intensity. This increase in available power allows for dramatic improvement in instrument scanning speed. In this letter we demonstrate imaging with 100 kHz pixel acquisition rates, yielding 10 images/s for 100×100 pixel images. Our maximum scan speed is limited by mechanical resonances in the microscope. We demonstrate that the optical signal to noise ratio is large enough to allow megahertz pixel acquisition rates. Such speeds make video rate (25 frames/s) imaging possible.

Etched fiber probes are fabricated using the process outlined by Hoffmann *et al.* The fiber is partially immersed in an etching solution consisting of 49% hydrofluoric acid covered with a thin layer of isoctane. After immersion for approximately 90 min, the probes are removed and rinsed with

de-ionized (DI) water and acetone. They are then metallized with 150 nm of aluminum, and examined under an optical microscope. The tips have taper angles of $\sim 30^\circ$, and the transmitted power through the probe is of order microwatts.

The unusually large optical throughput is attributed to the fact that chemical etching preserves the integrity of the fiber core to within a few microns of the aperture. In conventional pulled fiber probes,⁷ both the cladding and the core are tapered simultaneously. The core becomes too small to support an optical mode hundreds of microns before the end of the fiber. Thus the optical mode fills the cladding and interacts with the metal coating long before the mode interacts with the aperture. By chemically etching the fiber, the integrity of the core is maintained to within a few microns of the end of the fiber. This leads to less interaction with the metal coating and higher optical throughput.

The near-field instrument used in these measurements is a transmission microscope fabricated at Yale University. The sample remains stationary while the tip is scanned using a piezoelectric tube scanner. We scan the tip rather than the sample since the resonance frequency of the tip assembly is much higher than the sample stage. This allows for faster scanning speeds. The height of the tip above the sample is controlled by shear-force⁸ techniques utilizing an oscillating quartz tuning fork.⁹ The sample consists of 100-nm-wide lines and spaces patterned from 10-nm-thick aluminum on a quartz substrate. Images are acquired by illuminating locally with the near-field probe, collecting the transmitted light with conventional optics, and detecting the signal with a standard PIN diode photodetector. The signal from the detector is recovered using a transimpedance amplifier followed by additional voltage gain. The light source is a helium-neon laser operating at 633 nm.

A typical image obtained using these tips is shown in Fig. 1(a). The image is 200×200 pixels, and pixels are acquired at 10 kHz. Line cuts oriented perpendicular to the direction of the lines/spaces can be modeled by convolving a square wave (sample response) with a Gaussian (approximate probe response function). Such an analysis yields an aperture diameter of order 70 nm.

Although the available bandwidth of our PIN diode extends out to 500 kHz, the maximum scan speed at which we can make reasonable images is limited by a mechanical resonance in our piezo scanner. This is documented in Fig. 1. The piezo resonance manifests itself as a distortion in the images as the rate at which single lines are acquired is in-

^{a)}Electronic mail: scott.bukofsky@yale.edu

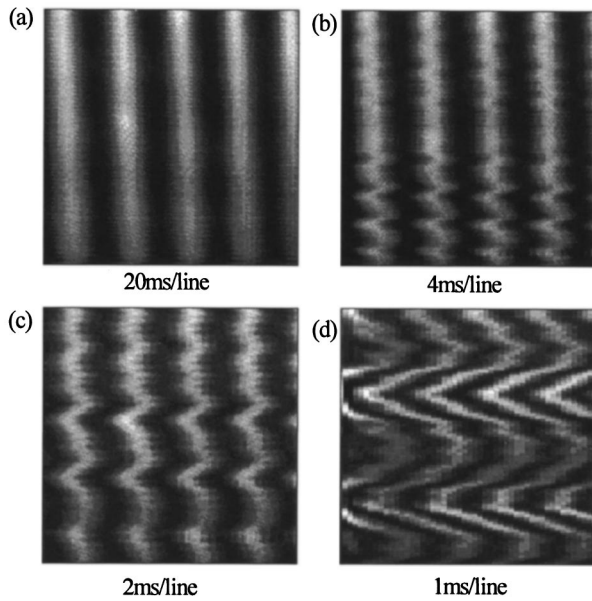


FIG. 1. Near-field transmission images as a function of scanning speed. The y axis is the fast scan direction. Images are 100 nm lines and spaces, pixels acquired at (a) 10 kHz, 200×200 pixels, (b) 50 kHz, 200×200 pixels, (c) 100 kHz, 200×200 pixels, and (d) 100 kHz, 100×100 pixels.

creased from 50 Hz to 1 kHz. At pixel acquisition rates as high as 100 kHz [Figs. 1(c) and 1(d)], the sample features are still well resolved but are distorted by the mechanical resonance. The observed frequency of oscillation agrees well with our known piezo resonance at 2.5 kHz.

Despite this mechanical limitation, there is ample optical signal to scan faster. Our data acquisition electronics can collect data as fast as 500 kHz, comparable to the bandwidth of the photodetector. The following simple experiment was performed to approximate what data would look like if the mechanical system could scan faster. The light source is modulated at 50 kHz using a photoelastic modulator. The light emitted from the near-field aperture is imaged directly onto the photodetector. Note that there is no sample and we are not scanning. Because losses associated with the photoelastic modulator reduce the maximum optical intensity we can launch onto the fiber, the power through the aperture is of order 200 nW. Figure 2 shows both the temporal and spectral photovoltage.

As shown in the inset to Fig. 2, the noise floor is flat across the spectral bandwidth and equal to $1.5 \text{ pW}/\sqrt{\text{Hz}}$. This is the Johnson noise of the $100 \text{ k}\Omega$ load resistor of our transimpedance amplifier after a subsequent voltage gain of 10, and a detector responsivity of 0.3 A/W . The sidebands at 25 kHz are a remnant of our modulation apparatus. The data in Fig. 2 document a signal to noise ratio of 190 while operating with a 500 kHz bandwidth. This bandwidth is made possible by the increased intensity from etched probes, and makes scanning at video rates feasible with good signal to noise ratio. To quantify what we mean by video rate, consider the issues of acquisition rate and signal to noise ratio. First, a 128×128 pixel image refreshed at 25 frames/s requires greater than 400 kHz signal bandwidth. This is consistent with our 500 kHz bandwidth. Second, the noise level in a system with n bits of dynamic range is of order the least significant bit. Our signal to noise ratio of 190 is consistent

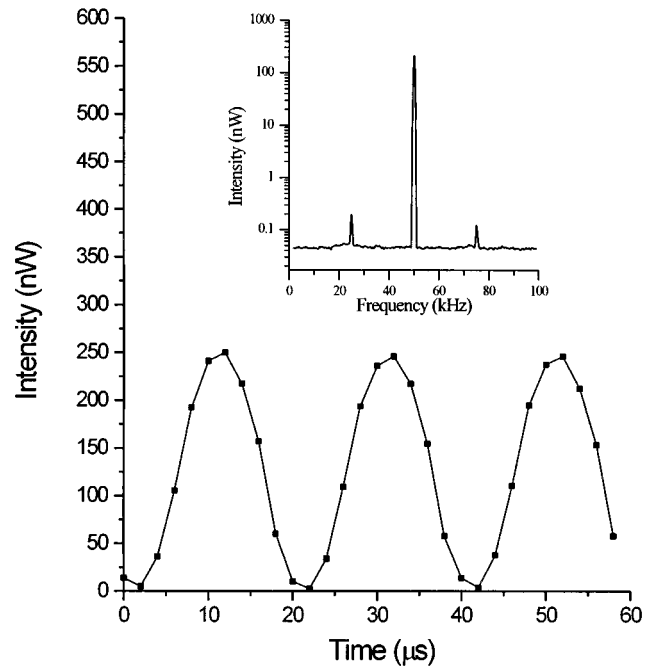


FIG. 2. Transmitted power from an etched fiber probe with laser source modulated at 50 kHz. Inset shows the power spectrum of the signal. The noise floor associated with the measurement is $1.5 \text{ pW}/\sqrt{\text{Hz}}$. This documents a signal to noise ratio of 190 at a pixel acquisition rate of 0.5 MHz.

with 7 or 8 bits of dynamic range. As discussed below, this performance is impossible to achieve with pulled fiber probes.

Within the context of a simple expression, one can quantify the signal to noise ratio as a function of optical power and signal bandwidth. Since optical power is measured by converting photocurrent into voltage by means of a resistor, the signal voltage is σPR , where σ is the responsivity of the photodiode in A/W , P is the power in W , and R is the resistance in Ω . There are two uncorrelated noise sources to consider: the Johnson noise of the resistor and the laser amplitude fluctuations. Therefore, the signal to noise (S/N) ratio is

$$S/N = \frac{\sigma PR}{\sqrt{4kTRB + (f\sigma PR)^2}}, \quad (1)$$

where k is Boltzman's constant, T is temperature, B is bandwidth, and f is the amount of laser amplitude fluctuation. It should be noted that P is the measured power at the detector and thus includes all system losses.

Figure 3 compares this expression with experimental data. The solid lines are Eq. (1) evaluated at several bandwidths with $\sigma = 0.3 \text{ A/W}$, $R = 100 \text{ k}\Omega$, and $f = 0.2\%$, consistent with our experimental apparatus. The data points (squares and triangles) are obtained by taking 2×10^4 samples of the photovoltage after filtering it with a variable bandwidth (30 and 300 kHz) low-pass filter. The S/N ratio is the mean of these data divided by their standard deviation. This figure emphasizes that the optimum S/N occurs when the optical power is large enough such that the laser fluctuation noise dominates the electronic noise. With the parameters given above, at least $1 \mu\text{W}$ is needed for best S/N. This power level cannot be achieved with conventional pulled fiber probes since heating effects¹⁰⁻¹² in the tip limit the avail-

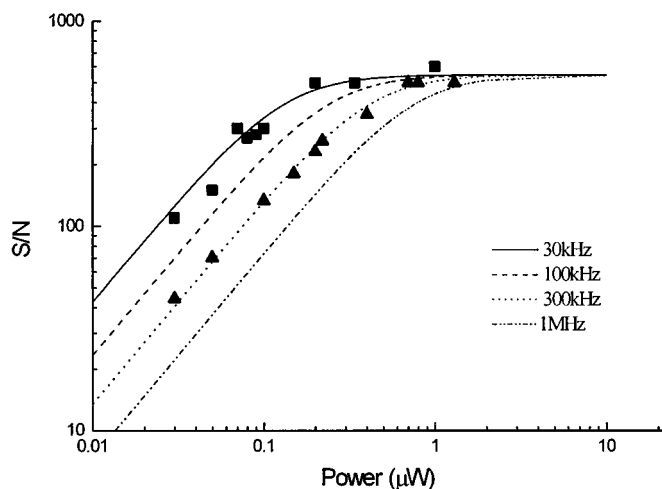


FIG. 3. Signal to noise ratio vs emitted power for several bandwidths. The lines are fits to the equation discussed in the text, using $R=100\text{ k}\Omega$, $\sigma=0.3\text{ A/W}$, and $f=0.2\%$. The points are measured values as a function of bandwidth: 30 kHz (squares) and 300 kHz (triangles).

able power to nanowatts. However, microwatt power levels are easily achieved using chemically etched fiber probes.

This calculation shows that NSOM is now a viable tool for video rate imaging. The enabling technology is the fabrication of chemically etched near-field fiber probes. Since the optical signal to noise now allows MHz pixel acquisition rates, issues related to mechanically scanning the probe above a sample at speeds approaching several mm/second need to be addressed.

First, the high scan speeds for video images place restrictions on the mechanical resonances of the instrument. Piezoelectric scanners in particular are prone to resonant behavior in the kHz regime. As discussed above, image distortion can be caused by the resonant response of the scanning system. Raster patterns with sharp turn-around points create the worst distortions. This is demonstrated in Fig. 4, which shows images of lines and spaces acquired with two different scan patterns. In Fig. 4(a), the tip traces out a standard serpentine raster pattern. The image shows distortions due to mechanical resonances. In Fig. 4(b) the tip moves up and down with a sinusoidal pattern, which eliminates the sharp turn-around points at the end of each line. In the latter case, the resonant effects have been removed. This experiment demonstrates that at high scanning speeds the scanning pattern is extremely important.

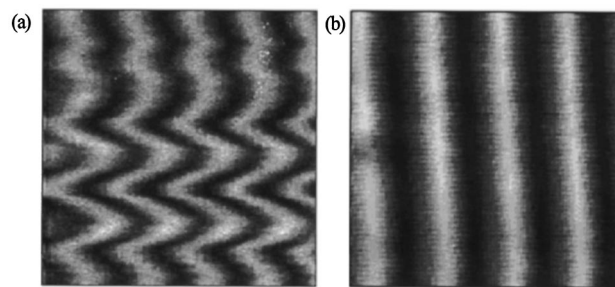


FIG. 4. Near-field transmission images as a function of scan pattern. Images consist of 200×200 pixels acquired at 50 kHz. In (a) the tip traces out a standard raster pattern, while in (b) the tip traces out a sinusoidal pattern, eliminating the sharp turn-around points at the end of each line. The y axis is the fast scan direction.

Second, it is not clear how topographic information can be obtained at speeds of mm/s. All of our data thus far were taken on essentially flat samples. Although shear-force techniques can control the tip-sample distance, they cannot adjust to height fluctuations at these high speeds. The response of shear-force feedback as it is presently implemented is limited to a few hundred hertz, and perhaps a few kilohertz for phase-sensitive techniques.¹³ If topographic information is required at video rates, a new paradigm in noncontact height control will have to be developed.

The authors would like to thank Khaled Karrai for bringing to our attention the work of Zeisel *et al.* This work was supported in part by the Semiconductor Research Corporation under Grant No. 96-LJ-438 and by the Army Research Office under Grant No. DAAH04-95-1-0368.

- ¹M. A. Paesler and P. J. Moyer, *Near-Field Optics* (Wiley, New York, 1996).
- ²D. W. Pohl, W. Denk, and M. Lanz, *Appl. Phys. Lett.* **44**, 651 (1984).
- ³E. Betzig, J. K. Trautman, T. D. Harris, J. S. Weiner, and R. L. Kostelak, *Science* **251**, 1468 (1991).
- ⁴L. Novotny, D. W. Pohl, and B. Hecht, *Opt. Lett.* **20**, 970 (1995).
- ⁵P. Hoffmann, B. Dutoit, and R.-P. Salathe, *Ultramicroscopy* **61**, 165 (1995).
- ⁶D. Zeisel, S. Nettesheim, B. Dutoit, and R. Zenobi, *Appl. Phys. Lett.* **68**, 2491 (1996).
- ⁷G. A. Valaskovic, M. Holton, and G. H. Morrison, *Appl. Opt.* **34**, 1215 (1995).
- ⁸E. Betzig, P. L. Finn, and J. S. Weiner, *Appl. Phys. Lett.* **60**, 2484 (1992).
- ⁹K. Karrai and R. D. Grober, *Appl. Phys. Lett.* **66**, 1842 (1995).
- ¹⁰D. I. Kavaljdjev, R. Toledo-Crow, and M. Vaez-Iravani, *Appl. Phys. Lett.* **67**, 2771 (1995).
- ¹¹A. H. LaRosa, B. I. Yakobsen, and H. D. Hallen, *Appl. Phys. Lett.* **67**, 2597 (1995).
- ¹²M. Stähelin, M. A. Bopp, G. Tarrach, A. J. Meixner, and I. Zschokke-Gränacher, *Appl. Phys. Lett.* **68**, 2603 (1996).
- ¹³W. A. Atia and C. C. Davis, *Appl. Phys. Lett.* **70**, 405 (1997).